Journal of Medicinal Chemistry

Article

pubs.acs.org/jmc

Dual Protonophore–Chitinase Inhibitors Dramatically Affect *O. volvulus* Molting

Major Gooyit,[†] Nancy Tricoche,[‡] Sara Lustigman,[‡] and Kim D. Janda*[,†]

[†]Departments of Chemistry and Immunology and Microbial Science, The Skaggs Institute for Chemical Biology, and The Worm Institute of Research and Medicine, The Scripps Research Institute, 10550 North Torrey Pines Road, La Jolla, California 92037, United States

[‡]Lindsley F. Kimball Research Institute, New York Blood Center, New York, New York 10065, United States

Supporting Information

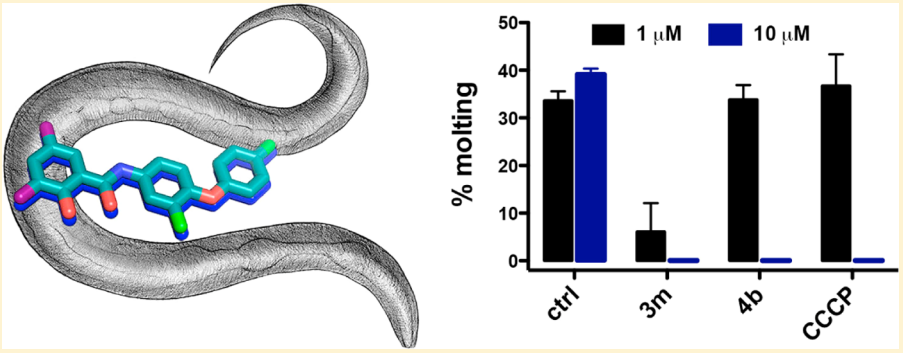

ABSTRACT: The L3-stage-specific chitinase OvCHT1 has been implicated in the development of *Onchocerca volvulus*, the causative agent of onchocerciasis. Closantel, a known anthelmintic drug, was previously discovered as a potent and specific OvCHT1 inhibitor. As closantel is also a known protonophore, we performed a simple scaffold modulation to map out the structural features that are relevant for its individual or dual biochemical roles. Furthermore, we present that either OvCHT1 inhibition or protonophoric activity was capable of affecting *O. volvulus* L3 molting and that the presence of both activities in a single molecule yielded more potent inhibition of the nematode's developmental process.

INTRODUCTION

Onchocerciasis, or river blindness, has plagued over 37 million people worldwide, occurring mostly in the sub-Saharan Africa, Yemen, and isolated areas of Central and South America.[1] The culprit for the infection is the filarial nematode *Onchocerca volvulus*, which is transmitted to humans through bites of infected blackflies of the genus *Simulium*. Initial pathological manifestations of the disease include inflammation of the skin and eyes caused by dead or dying microfilariae that eventually results to skin lesions and blindness. Currently, the antiparasitic agent ivermectin is the only drug available for mass treatment.[2] While the drug has proven to be effective in reducing morbidity by killing the microfilariae, it does not target the adult worms and thus does not completely eliminate parasite transmission and infection.[3,4] Additionally, the emergence of ivermectin-resistant *O. volvulus*[5,6] further necessitates the need to develop therapeutic strategies for the treatment of onchocerchiasis.

Molting is a crucial feature in the life cycle of *O. volvulus*. The shedding of the L3 cuticle during ecdysis and the proteolytic remodeling of the new L4 cuticle is particularly important for the transition between hosts and infection process of the parasitic nematode. Chitinases act in concert with chitin synthases to facilitate chitin metabolism, a significant process for nematode development.[7] Chitinases have been implicated in remodeling processes during filarial molting and egg hatching.[8,9] In the rodent filarial nematode *Acanthocheilonema viteae*, RNA interference studies targeting the chitinase gene significantly inhibited the molting of L3 worms.[10] A chitinase from *O. volvulus*, OvCHT1, was recently identified and found to be solely expressed within the glandular esophagus of the infective L3 larvae and is secreted during postinfective development.[11] OvCHT1 was hypothesized to play roles in molting and parasite transmission and, as such, presents a potential target for pharmacological intervention. From our previous screening efforts, we had disclosed a known veterinary anthelmintic drug, closantel (**1**), which exhibits potent and selective inhibition toward OvCHT1 (IC_{50} = 1.60 ± 0.08 μM, K_i = 0.47 ± 0.08 μM).[12] As closantel is a known uncoupler of oxidative phosphorylation,[13] our recent findings implicated a potential bimodal action of the drug. Furthermore, closantel was shown to inhibit the molting of *O. volvulus* L3 to L4 larvae at 100 μM;[12] however, this profound effect on filarial molting was unclear as to whether it was due to inhibition of OvCHT1 or uncoupling of mitochondrial activity. In the same study, a "retro-fragment"-based approach was conducted to unravel the

Received: April 24, 2014
Published: June 11, 2014

   dx.doi.org/10.1021/jm5006435 | *J. Med. Chem.* 2014, 57, 5792–5799

molecular frameworks that are required for closantel's chitinase inhibitory activity, in which compound **2** was identified as the relevant structural fragment with a comparable potency as that of closantel (IC_{50} = 5.8 ± 0.3 μM).[12]

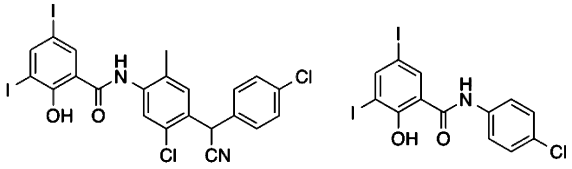

In this study, we constructed a series of closantel analogues to deduce the molecular features that are critical for chitinase inhibition and mitochondrial-uncoupling activity. Because the 3,5-diiodosalicylate moiety is key to closantel's binding specificity by anchoring it within the OvCHT1 active site,[14] we retained this fragment and focused on scaffold expansion of **2** to generate analogues **3**, **4**, and **5** (which were easily accessed through amide coupling of carboxylic acids **6** and amine reactants, Figure 1). Simple structural modifications led to the

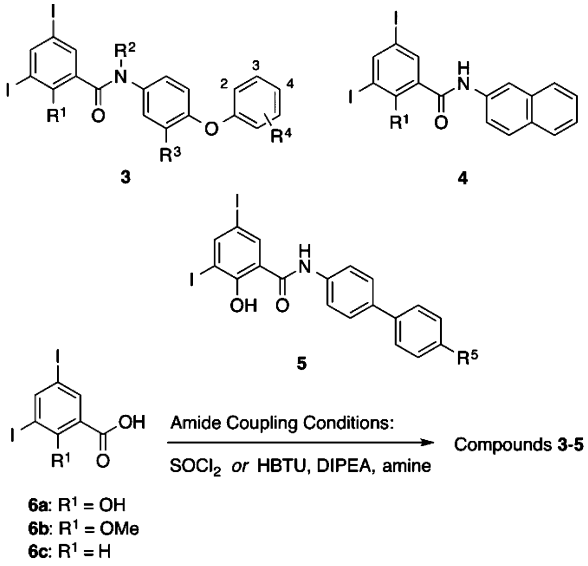

Figure 1. Structures and preparation of closantel analogues.

identification of more potent compounds with dual modes of action (as an OvCHT1 inhibitor and a protonophore) as well as analogues acting as chitinase inhibitors only. We also demonstrate that while either OvCHT1 inhibition or mitochondrial uncoupling was effective in abrogating the L3-to-L4 molt, synergistic activities incorporated into a single molecule afforded a more profound impact on molting.

RESULTS AND DISCUSSION

***O. volvulus* Chitinase Inhibition.** The presence of additional (phenolic and amide) protons in closantel may be key for its dual mode of action. For instance, the hydrogen-bonding moieties may be important to affect the required acidic residues of the chitinase catalytic site.[15] To elucidate the relevance of these protons, we initially prepared a simplified version of closantel using a phenoxyphenyl scaffold (compound **3a**) and its analogues containing methyl substituents in place of the key hydrogens (compounds **3b**–**d**). As shown in Table 1, compounds **3a**, **3b**, and **3c** have comparable chitinase inhibitory

Table 1. IC_{50} of *O. volvulus* Chitinase Inhibition

compd	R^1	R^2	R^3	R^4	R^5	IC_{50} (μM)
1						1.60 ± 0.08
3a	OH	H	H	H		1.98 ± 0.13
3b	OMe	H	H	H		1.28 ± 0.19
3c	OH	Me	H	H		1.81 ± 0.18
3d	OMe	Me	H	H		3.71 ± 0.14
3e	H	H	H	H		1.06 ± 0.08
3f	OH	H	H	4-Me		1.11 ± 0.03
3g	OH	H	H	4-F		1.57 ± 0.09
3h	OH	H	H	4-Cl		0.70 ± 0.02
3i	OMe	H	H	4-Cl		0.60 ± 0.07
3j	H	H	H	4-Cl		0.87 ± 0.10
3k	OH	H	H	3-Cl		1.74 ± 0.09
3l	OH	H	H	2-Cl		1.20 ± 0.17
3m	OH	H	Cl	4-Cl		0.34 ± 0.04
4a	OH					0.94 ± 0.05
4b	OMe					0.89 ± 0.10
4c	H					1.29 ± 0.03
5a					H	0.47 ± 0.03
5b					Me	0.99 ± 0.16
5c					Cl	0.37 ± 0.03

profile as closantel, indicating that the phenolic or amide proton is not necessary for chitinase inhibition. However, simultaneous substitution of both hydrogens with methyl groups (as in the case of compound **3d**) resulted to a 2-fold decrease in potency. Exclusion of the hydroxyl moiety (compound **3e**) led to a slight increase in inhibitory activity with an IC_{50} value of 1.06 ± 0.08 μM.

In an effort to increase the potency against OvCHT1, we constructed a series of derivatives based on compound **3a**. From Table 1, it is evident that introduction of the chloro substituent at the *para*-position of the terminal phenyl ring (compound **3h**) enhanced the potency almost 3-fold relative to **3a**. The similar IC_{50} values of compounds **3i**, **3j**, and **3h** further confirmed that neither the phenolic proton nor the hydroxyl functionality is important for chitinase inhibition. Inclusion of a chloro-substituent in the middle phenyl ring (compound **3m**, also known as rafoxanide and a known veterinary anthelmintic drug)[16] further improved the potency with an IC_{50} value of 0.34 ± 0.03 μM and a competitive inhibitory constant (K_i) of 0.13 ± 0.01 μM. We then prepared naphthyl analogues **4a**–**c** and biphenyl compounds **5a**–**c** in an attempt to establish favorable π-stacking and van der Waals interaction with the hydrophobic residues within the chitinase active site to optimize OvCHT1 inhibition. Biphenyl scaffolds have been previously considered as privileged substructures that preferentially interact with diverse proteins.[17] Interestingly, we did observe enhanced potency with the biaryl compounds **4** and **5**, with IC_{50} values for OvCHT1 inhibition as low as 0.37 ± 0.03 μM (for compound **5c**). Select compounds that exhibited good potency against OvCHT1 were also evaluated for inhibition of chitinases from other species. Compounds **3h**, **3i**, **3j**, **3m**, **5a**, and **5c** (each at a final concentration of 10 μM) showed complete inhibition of OvCHT1 (see Figure S1 in the Supporting Information) while sparing other chitinases including those from another filarial nematode *Brugia malayi* (BmCHT1) and protozoans *Entamoeba histolytica* (EhCHT1) and *Plasmodium falciparum* (PfCHT1). These results indicate that the analogues are highly OvCHT1-specific and thus are

dx.doi.org/10.1021/jm5006435 | J. Med. Chem. 2014, 57, 5792–5799

amenable for evaluation in chitinase-specific diseases such as onchocerciasis.

Evaluation of Protonophoric Activity. To examine mitochondrial-uncoupling activity, compounds **1**−**5** were tested using tetramethylrhodamine ethyl ester (TMRE), a positively charged, mitochondrion-selective dye that serves as a membrane potential sensor. In the presence of a protonophore (e.g., carbonyl cyanide *m*-chlorophenyl hydrazone or CCCP), the mitochondrion gets depolarized and thus fails to sequester TMRE, resulting in decreased fluorescence intensity. A microplate fluorescence assay was developed to monitor mitochondrial uncoupling of HEK-293T/17 cells in the presence of the inhibitors. Following incubation with the inhibitors at 37 °C, the cells were stained with TMRE and subsequently analyzed by fluorescence spectrometry. As depicted in Figure 2, a dissociable proton (i.e., phenolic

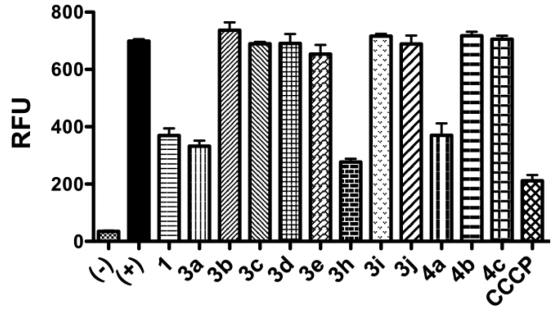

Figure 2. Evaluation of mitochondrial-uncoupling activity using a microplate fluorescence assay. HEK 293T/17 cells were incubated with compound (50 μM) and subsequently stained with TMRE. Data shown as mean fluorescence intensity ± sd (n = 3). Unstained cells (no TMRE) and DMSO were used as negative (−) and positive (+) controls, respectively. RFU = relative fluorescence units (λ_{ex} = 488 nm, λ_{em} = 575 nm).

hydrogen as in **1**, **3a**, **3h**, and **4a**) for the salicylanilide class of compounds is critical for mitochondrial-uncoupling activity. As expected, removal of the hydroxyl moiety (as in compounds **3e**, **3j**, and **4c**) or masking it with a methyl group (compounds **3b**, **3i**, **3d**, and **4b**) resulted to a loss of uncoupling activity. We note, however, that the amide proton is equally significant, as substituting it with a methyl group while retaining the hydroxyl moiety (like in the case of compound **3c**) eradicated protonophoric activity. Results of mitochondrial-uncoupling activity for the other compounds listed in Table 1 are given in Supporting Information Figure S2. Separate experiments using flow cytometry to analyze membrane polarization were also conducted and the results (see Figure S3 in the Supporting Information) were in agreement to those obtained from the microplate fluorescence assay.

From the series of derivatives listed in Table 1, we have identified more potent analogues with dual biochemical roles (both as a chitinase inhibitor and a proton ionophore) as well as compounds with chitinase inhibitory activity only. Compounds **3m** proved to be the most potent OvCHT1 inhibitor with good mitochondrial-uncoupling activity, while compounds **3i**, **3j**, and **4b** displayed similar chitinase inhibition profile but devoid of protonophoric activity.

Bioaccumulation in the Model Nematode *C. elegans*. In general, nematodes are resistant to perturbation of small molecules due to the thick cuticles that line their exteriors and oral and rectal cavities.[18,19] The highly insoluble cuticle of *O. volvulus* is a collagenous framework of proteins that are cross-linked by disulfide bridges.[20] As the bioaccumulation of a drug is correlated to its bioactivity, we deemed it important to investigate the penetrability of the compounds in the nematode. The limited availability of *O. volvulus*, however, prompted us to consider an alternative model organism, the soil nematode *Caenorhabditis elegans*. The cuticle of adult *C. elegans* is composed of multiple layers of collagenous extracellular structures[18] and thus resemble the physical barriers of other nematodes. In fact, due to its easy culturability and rapid life cycle, it was previously used as a model system of bioaccumulation to identify small bioactive molecules.[21] Using a similar approach to address nematode permeability, we initially incubated late-stage L4 worms with compounds **1**, **3h**, **3i**, **3j**, **3m**, **4a**, **4b**, **5a**, **5c**, and CCCP (each at 10 μM final concentration, and equivalent to 2 nmol/mg worm) for 6 h. By LC-MS analysis of worm homogenates, we determined that all the aforementioned compounds accumulated in *C. elegans*. *C. elegans* is also equipped with enzymatic xenobiotic defenses that add to its resistance to exogenous pharmacologicals.[22] Similar to what was observed in cattle and sheep,[23] the primary, albeit minor, metabolic pathway of closantel in *C. elegans* is reductive deiodination, resulting in the formation of two monoiodoclosantel isomers (see Figure S4 in the Supporting Information). Sulfation, glycosylation, and glucuronidation of the salicylate moiety of closantel were not observed in *C. elegans* homogenates. We add that no effect on the viability of the L4 worms was observed upon incubation with the compounds. We then set out to quantify the concentration of representative compounds in the nematode after 6 and 12 h of incubation. As indicated in Figure 3, compound **3m** displayed excellent

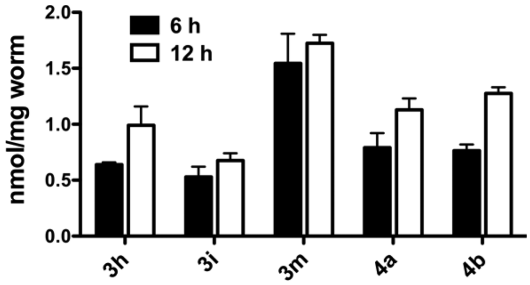

Figure 3. Bioaccumulation of chitinase inhibitors in *C. elegans*. Late-stage L4 worms were incubated with 10 μM inhibitor (equivalent to 2 nmol/mg worm) for 6 and 12 h. Data shown as mean concentration ± sd (n = 3), expressed in nmol/mg worm.

bioaccumulation in *C. elegans*, with worm levels of 1.55 ± 0.37 and 1.73 ± 0.11 nmol/mg at 6 and 12 h, respectively, which were >75% of the initial dose of the compound to worms. The concentrations of the naphthyl analogues **4a** and **4b** were a little less than 50% of the dose at 6 h, and increased to 1.13 ± 0.14 and 1.28 ± 0.08 nmol/mg, respectively, after 12 h. The inability to accumulate at adequate concentrations within the worm can render the compound ineffective no matter how potent it is against the target in vitro. In a survey of over 1000 drug-like small molecules, only less than 10% were shown to penetrate *C. elegans* at concentrations >50% of the initial doses.[21] Thus, the findings that we observed for the closantel analogues are encouraging because they readily accumulate within the nematode at high levels. We surmise that these compounds also accumulate in the filarial nematode *O. volvulus*

dx.doi.org/10.1021/jm5006435 | J. Med. Chem. 2014, 57, 5792−5799

and thus increase the likelihood of interaction with the target protein OvCHT1.

Inhibition of *O. volvulus* L3Molting. The target protein OvCHT1 is expressed predominantly in the infective L3 larvae and may be critical in the molting and development of the nematode.[11] Filarial molting of *O. volvulus* L3 larvae is typically assayed by incubation of the larvae in complete growth medium in the presence of peripheral blood mononuclear cells (PBMCs). To evaluate the efficacy of the inhibitors based solely on their inhibitory properties, the L3 larvae were initially incubated with select compounds (10 μM) for 24 h (to allow sufficient time for accumulation) prior to addition of the growth medium and PBMCs and monitored until day 6 when molting was assessed. Under this assay condition, compounds **3h**, **3m**, and **4a** (all have dual protonophoric and chitinase inhibitory activities) completely abolished molting at 10 μM, as indicated in Figure 4A. Significant effects on molting (up to

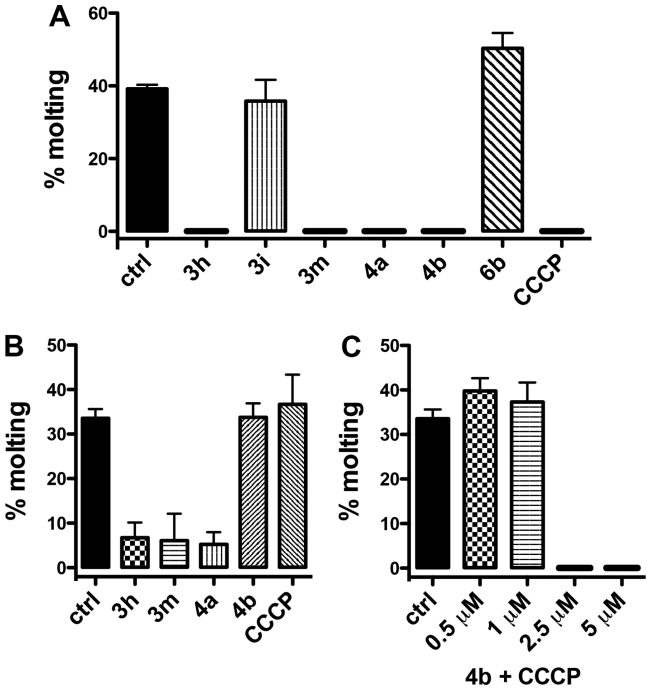

Figure 4. Molting of *O. volvulus* L3 larvae in the presence of inhibitors. Percent molting at (A) 10 μM and (B) 1 μM inhibitor concentration, and (C) in the presence of 1:1 combination of **4b** and CCCP each at concentrations shown. Data presented as percent molting in a total of 10 wells containing on average 5−10 larvae per well.

84% inhibition) were also observed at a lower concentration of 1 μM for compounds **3h**, **3m**, and **4a** (Figure 4B). Of note, no considerable effect on cell viability was observed when HEK 293T/17 cells were treated with 1 and 10 μM of **3h**, **3m**, or **4a**, for 24 h (see Figure S5 in the Supporting Information). Treatment of L3 larvae with compound **6b** (neither an OvCHT1 inhibitor nor a protonophore), showed no inhibition on molting (Figure 4A). To ascertain which activity is relevant for inhibition, we also evaluated compounds **3i** and **4b** (chitinase inhibitors only) and CCCP (a protonophore only) for their impact on L3 molting. Compounds **3i** and **4b** have differing effects; while **4b** inhibited molting at 10 μM, only marginal inhibition was observed with **3i** at the same inhibitor concentration (Figure 4A). The difference in efficacy between the two compounds at 10 μM could not be readily explained as both display similar IC_{50} values against OvCHT1; however, compound **4b** could be accumulating within *O. volvulus* at higher levels, as was observed in the *C. elegans* model (vide supra), which might account for its better activity. At a higher concentration of 100 μM, compound **3i** completely hindered L3 molting. CCCP also fully inhibited the molting of L3 larvae at 10 μM, suggesting that mitochondrial-uncoupling, by itself, affects this developmental process. Many of the proteins that are necessary for *O. volvulus* L3 molting are stored within the granules of the esophageal glands.[24] Mitochondrial-uncoupling in the glandular esophagus may, therefore, affect the synthesis of key proteins (including OvCHT1) that are essential for larval development. At a final concentration of 1 μM, both **4b** and CCCP did not show any impact on molting (Figure 4B). As both chitinase inhibitory and protonophoric activities are likely required for more potent inhibition, we investigated the effect of incubating L3 larvae with a 1:1 mixture of **4b** and CCCP. Whereas **3h**, **3m**, and **4a** were effective at 1 μM, no effect on molting was observed using a combination of **4b** + CCCP at 0.5 or 1 μM of each compound (Figure 4C). Treatment with 2.5 μM each of **4b** and CCCP was sufficient to completely suppress the L3-to-L4 molt.

Combination therapy, the simultaneous use of two or more drugs with distinct modes of action and biological targets, has been exploited as a treatment modality in several diseases including HIV,[25] metastatic melanoma,[26] second-stage *Trypanosoma brucie gambiense* sleeping sickness,[27] and malaria.[28] Despite its efficacy in improving response to medication and minimizing drug resistance, combination therapy is resource-intensive, complicated to administer, and prone to drug−drug interactions and adverse side effects. The utility of "combi-molecules" or single agents with polypharmacological targets has emerged as an alternative strategy, displaying the same advantages while bypassing the drawbacks of drug combinations. The combi-targeting concept is a growing field of interest in the search for therapies against cancer[29,30] and infectious diseases.[31] This dual inhibition approach is well exemplified by compounds **3h**, **3m**, and **4a**, which, through concomitant uncoupling of oxidative phosphorylation and inhibition of OvCHT1, resulted in a more robust inhibition of *O. volvulus* molting. Moreover, our results demonstrate the superior activity of the dual-targeted single molecules over monotherapy or a dual drug combination (**4b** + CCCP).

■ CONCLUSION

The implications of OvCHT1 in filarial molting has opened an avenue to develop strategies toward the elimination of onchocerciasis. Earlier, DNA immunization with OvCHT1 was shown to provide significant protection against the developing L3 larvae in mice; however, large and frequent doses of DNA were needed to attain the result.[32] The efficacy of the dual mechanistic drug, closantel, has steered us to prepare analogues to further probe the individual effects of OvCHT1 inhibition and protonophoric activity on *O. volvulus* L3 molting. By subtle structural modifications, we have identified potent bifunctional analogues (**3h**, **3m**, and **4a**) as well as OvCHT1 inhibitors only (**3i** and **4b**). These compounds were also found to readily bioaccumulate in the model nematode *C. elegans* at concentrations up to >75% of the initial dose to worms. Moreover, our results have clearly established the significance of each biochemical role in modulating the *O. volvulus* L3-to-L4 molt and that synergistic activities (as displayed by **3h**, **3m**, and **4a**) provided a

dx.doi.org/10.1021/jm5006435 | *J. Med. Chem.* 2014, 57, 5792−5799

formidable impact on molting. Although these strategies will still need to be validated as potential antifilarial therapies, what we have presented thus far is a notch closer toward the search for effective treatments to combat onchocerciasis.

EXPERIMENTAL SECTION

Chemistry. General Information. All reactions were performed under nitrogen atmosphere unless otherwise noted. ^{1}H and ^{13}C NMR spectra were recorded on a Bruker DRX-500 or Bruker DRX-600 equipped with a 5 mm DCH cryoprobe. All carboxylic acid and amine starting reactants were obtained from commercial sources except for compounds **6b** (used for the syntheses of compounds **3b**, **3d**, **3i**, and **4b**), **6c** (prepared as described previously[33] and used for syntheses of compounds **3e**, **3j**, and **4c**) and *N*-methyl-4-phenoxyaniline **7** (used for the syntheses of compounds **3c** and **3d**).

Compounds **3**−**5** were prepared according to general procedure A or B.

General Procedure A. A mixture of 3,5-diiodosalicylic acid (1.0 equiv) and thionyl chloride (5 equiv) was heated under reflux for 7 h. After concentration under reduced pressure, cold hexanes were added to precipitate the acid chloride product. The residue was filtered, washed several times with cold hexanes, and air-dried. A solution of the amine reactant (1.0 equiv) and DIPEA (3 equiv) in DMF was added to the acid chloride, and the resulting mixture was stirred at rt for 1 h. The product was subsequently subjected to preparative HPLC purification.

General Procedure B. A solution of **6b** or **6c** (1.0 equiv), DIPEA (2.0 equiv) and HBTU (1.1 equiv) in DMF was stirred for 15 min at rt. The amine reactant (1.0 equiv) was added, and the resulting mixture was stirred overnight at rt. The product was isolated by preparative HPLC purification. Purity of the final products are generally >95% as assessed by HPLC.

*2-Hydroxy-3,5-diiodo-N-(4-phenoxyphenyl)benzamide (**3a**).* Procedure A, 53% yield. ^{1}H NMR (500 MHz, DMSO-d_6) δ 6.99−7.10 (m, 4H), 7.14 (t, J = 7.39 Hz, 1H), 7.36−7.44 (m, 2H), 7.64−7.71 (m, 2H), 8.23 (d, J = 1.90 Hz, 1H), 8.40 (d, J = 1.86 Hz, 1H), 10.66 (s, 1H). ^{13}C NMR (151 MHz, DMSO-d_6) δ 81.7, 89.1, 117.3, 118.4, 119.0, 123.4, 123.8, 130.1, 132.8, 135.8, 149.7, 153.5, 156.9, 159.5, 166.7. HRMS-ESI (m/z): [M + H]$^+$ calcd for $C_{19}H_{14}I_2NO_3$, 557.9058; found, 557.9058.

*3,5-Diiodo-2-methoxy-N-(4-phenoxyphenyl)benzamide (**3b**).* Procedure B, 60% yield. ^{1}H NMR (600 MHz, $CDCl_3$) δ 3.91 (s, 3H), 6.95−7.05 (m, 4H), 7.10 (t, J = 7.38 Hz, 1H), 7.33 (t, J = 7.94 Hz, 2H), 7.61 (d, J = 8.84 Hz, 2H), 8.24 (d, J = 2.12 Hz, 1H), 8.38 (d, J = 2.13 Hz, 1H), 9.38 (s, 1H). ^{13}C NMR (151 MHz, $CDCl_3$) δ 62.7, 90.1, 93.8, 118.7, 119.8, 121.9, 123.4, 129.4, 129.9, 133.2, 141.3, 150.5, 154.2, 157.1, 157.5, 160.9. HRMS-ESI (m/z): [M + H]$^+$ calcd for $C_{20}H_{16}I_2NO_3$, 571.9214; found, 571.9213.

*2-Hydroxy-3,5-diiodo-N-methyl-N-(4-phenoxyphenyl)benzamide (**3c**).* Procedure A, 23% yield. ^{1}H NMR (600 MHz, $CDCl_3$) δ 3.47 (s, 3H), 6.92−7.02 (m, 3H), 7.02−7.09 (m, 4H), 7.13 (t, J = 7.38 Hz, 1H), 7.35 (t, J = 7.91 Hz, 2H), 7.92 (d, J = 1.63 Hz, 1H), 11.89 (s, 1H). ^{13}C NMR (151 MHz, $CDCl_3$) δ 39.7, 79.2, 87.6, 117.7, 119.3, 120.3, 124.0, 128.1, 130.1, 139.2, 139.4, 149.2, 156.8, 157.1, 159.5, 169.2. HRMS-ESI (m/z): [M + H]$^+$ calcd for $C_{20}H_{16}I_2NO_3$, 571.9214; found, 571.9205.

*3,5-Diiodo-2-methoxy-N-methyl-N-(4-phenoxyphenyl)-benzamide (**3d**).* Procedure B, 58% yield. ^{1}H NMR (600 MHz, $CDCl_3$) δ 3.46 (s, 3H), 3.88 (s, 3H), 6.82 (d, J = 8.78 Hz, 2H), 6.90 (d, J = 7.85 Hz, 2H), 7.01 (d, J = 8.78 Hz, 2H), 7.10 (t, J = 7.40 Hz, 1H), 7.29−7.40 (m, 4H), 7.93 (d, J = 1.98 Hz, 1H). ^{13}C NMR (151 MHz, $CDCl_3$) δ 37.5, 62.7, 87.6, 93.3, 118.9, 119.5, 123.7, 128.3, 130.0, 133.9, 137.4, 138.1, 147.6, 155.9, 156.3, 157.0, 166.7. HRMS-ESI (m/z): [M + H]$^+$ calcd for $C_{21}H_{18}I_2NO_3$, 585.9376; found, 585.9366.

*3,5-Diiodo-N-(4-phenoxyphenyl)benzamide (**3e**).* Procedure B, 45% yield. ^{1}H NMR (600 MHz, $CDCl_3$) δ 6.98−7.05 (m, 4H), 7.11 (t, J = 7.40 Hz, 1H), 7.31−7.37 (m, 2H), 7.56 (d, J = 8.73 Hz, 2H), 7.71 (s, 1H), 8.12 (s, 2H), 8.22 (t, J = 1.39 Hz, 1H). ^{13}C NMR (151 MHz, $CDCl_3$) δ 95.2, 118.9, 119.7, 122.3, 123.5, 129.9, 132.7, 135.4, 138.3, 148.4, 154.5, 157.4, 162.7. HRMS-ESI (m/z): [M + H]$^+$ calcd for $C_{19}H_{14}I_2NO_2$, 541.9109; found, 541.9106.

*2-Hydroxy-3,5-diiodo-N-(4-(p-tolyloxy)phenyl)benzamide (**3f**).* Procedure A, 51% yield. ^{1}H NMR (600 MHz, $CDCl_3$) δ 2.34 (s, 3H), 6.91−6.95 (m, 2H), 6.98−7.04 (m, 2H), 7.15 (d, J = 8.25 Hz, 2H), 7.44−7.50 (m, 2H), 7.78 (d, J = 1.89 Hz, 1H), 7.87 (s, 1H), 8.18 (d, J = 1.89 Hz, 1H). ^{13}C NMR (151 MHz, $CDCl_3$) δ 20.9, 77.2, 80.3, 89.0, 116.7, 118.9, 119.3, 123.5, 130.5, 130.7, 133.5, 134.3, 151.1, 154.5, 156.0, 160.4, 166.4. HRMS-ESI (m/z): [M + H]$^+$ calcd for $C_{20}H_{16}I_2NO_3$, 571.9220; found, 571.9215.

*N-(4-(4-Fluorophenoxy)phenyl)-2-hydroxy-3,5-diiodobenzamide (**3g**).* Procedure A, 43% yield. ^{1}H NMR (600 MHz, $CDCl_3$) δ 6.96−7.08 (m, 6H), 7.49 (d, J = 8.84 Hz, 2H), 7.79 (d, J = 1.44 Hz, 1H), 7.92 (s, 1H), 8.19 (d, J = 1.72 Hz, 1H). ^{13}C NMR (151 MHz, $CDCl_3$) δ 80.3, 89.0, 116.6 (d, J = 23.3 Hz), 116.7, 118.9, 120.8 (d, J = 8.26 Hz), 123.6, 131.1, 134.3, 151.1, 152.7 (d, J = 2.49 Hz), 155.7, 159.1 (d, J = 242.8 Hz), 160.4, 166.5. HRMS-ESI (m/z): [M + H]$^+$ calcd for $C_{19}H_{13}FI_2NO_3$, 575.8963; found, 575.8957.

*N-(4-(4-Chlorophenoxy)phenyl)-2-hydroxy-3,5-diiodobenzamide (**3h**).* Procedure A, 46% yield. ^{1}H NMR (600 MHz, DMSO-d_6) δ 7.01−7.08 (m, 2H), 7.07−7.14 (m, 2H), 7.41−7.50 (m, 2H), 7.65−7.74 (m, 2H), 8.23 (d, J = 1.80 Hz, 1H), 8.40 (d, J = 1.80 Hz, 1H), 10.69 (s, 1H). ^{13}C NMR (151 MHz, DMSO-d_6) δ 81.8, 89.1, 117.4, 119.3, 120.0, 123.8, 127.1, 129.9, 133.2, 135.8, 149.7, 153.0, 155.9, 159.5, 166.7. HRMS-ESI (m/z): [M + H]$^+$ calcd for $C_{19}H_{13}ClI_2NO_3$, 591.8668; found, 591.8660.

*N-(4-(4-Chlorophenoxy)phenyl)-3,5-diiodo-2-methoxybenzamide (**3i**).* Procedure B, 23% yield. ^{1}H NMR (600 MHz, $CDCl_3$) δ 3.91 (s, 3H), 6.92−6.96 (m, 2H), 7.01−7.05 (m, 2H), 7.27−7.31 (m, 2H), 7.60−7.66 (m, 2H), 8.26 (d, J = 2.20 Hz, 1H), 8.39 (d, J = 2.20 Hz, 1H), 9.40 (s, 1H). ^{13}C NMR (151 MHz, $CDCl_3$) δ 62.7, 90.1, 93.8, 119.9, 119.9, 122.0, 128.4, 129.3, 129.9, 133.6, 141.3, 150.6, 153.7, 156.2, 157.1, 160.9. HRMS-ESI (m/z): [M + H]$^+$ calcd for $C_{20}H_{15}ClI_2NO_3$, 605.8824; found, 605.8817.

*N-(4-(4-Chlorophenoxy)phenyl)-3,5-diiodobenzamide (**3j**).* Procedure A, 44% yield. ^{1}H NMR (600 MHz, $CDCl_3$) δ 6.92−6.97 (m, 2H), 6.99−7.04 (m, 2H), 7.28−7.32 (m, 2H), 7.57 (d, J = 8.78 Hz, 2H), 7.71 (s, 1H), 8.10−8.15 (m, 2H), 8.22 (t, J = 1.35 Hz, 1H). ^{13}C NMR (151 MHz, $CDCl_3$) δ 95.2, 119.8, 120.0, 122.4, 128.5, 129.9, 133.1, 135.4, 138.3, 148.4, 154.0, 156.1, 162.7. HRMS-ESI (m/z): [M − H]$^-$ calcd for $C_{17}H_{10}I_2NO_2$, 573.8568; found, 573.8556.

*N-(4-(3-Chlorophenoxy)phenyl)-2-hydroxy-3,5-diiodobenzamide (**3k**).* Procedure A, 43% yield. ^{1}H NMR (600 MHz, $CDCl_3$) δ 6.88−6.93 (m, 1H), 7.00 (t, J = 2.12 Hz, 1H), 7.04−7.08 (m, 2H), 7.08−7.12 (m, 1H), 7.23−7.29 (m, 1H), 7.52−7.58 (m, 2H), 7.80 (d, J = 1.83 Hz, 1H), 7.92 (s, 1H), 8.20 (d, J = 1.85 Hz, 1H). ^{13}C NMR (151 MHz, $CDCl_3$) δ 80.4, 89.1, 116.7, 116.9, 119.1, 120.1, 123.5, 123.7, 130.8, 131.9, 134.3, 135.3, 151.2, 154.3, 158.1, 160.4, 166.5. HRMS-ESI (m/z): [M + H]$^+$ calcd for $C_{19}H_{13}ClI_2NO_3$, 591.8668; found, 591.8663.

*N-(4-(2-Chlorophenoxy)phenyl)-2-hydroxy-3,5-diiodobenzamide (**3l**).* Procedure A, 35% yield. ^{1}H NMR (600 MHz, $CDCl_3$) δ 6.98−7.02 (m, 2H), 7.03 (dd, J = 1.40, 8.13 Hz, 1H), 7.12 (td, J = 1.44, 7.80 Hz, 1H), 7.23−7.25 (m, 1H), 7.48 (dd, J = 1.54, 8.00 Hz, 1H), 7.49−7.53 (m, 2H), 7.78 (d, J = 1.88 Hz, 1H), 7.87 (s, 1H), 8.19 (d, J = 1.87 Hz, 1H). ^{13}C NMR (151 MHz, $CDCl_3$) δ 80.3, 89.0, 116.7, 118.5, 121.2, 123.5, 125.3, 126.2, 128.2, 131.1, 131.3, 134.3, 151.2, 152.3, 155.0, 160.4, 166.4. HRMS-ESI (m/z): [M + H]$^+$ calcd for $C_{19}H_{13}ClI_2NO_3$, 591.8668; found, 591.8662.

*2-Hydroxy-3,5-diiodo-N-(naphthalen-2-yl)benzamide (**4a**).* Procedure A, 27% yield. ^{1}H NMR (600 MHz, DMSO-d_6) δ 7.46−7.51 (m, 1H), 7.51−7.55 (m, 1H), 7.78 (dd, J = 2.08, 8.86 Hz, 1H), 7.91 (d, J = 8.58 Hz, 2H), 7.95 (d, J = 8.90 Hz, 1H), 8.25 (d, J = 1.81 Hz, 1H), 8.30 (d, J = 1.61 Hz, 1H), 8.48 (d, J = 1.80 Hz, 1H), 10.84 (s, 1H). ^{13}C NMR (151 MHz, DMSO-d_6) δ 81.9, 89.2, 117.6, 118.8, 121.7, 125.5, 126.6, 127.5, 127.6, 128.3, 130.6, 133.1, 134.9, 136.0, 149.7, 159.5, 167.0. HRMS-ESI (m/z): [M − H]$^-$ calcd for $C_{17}H_{10}I_2NO_2$, 513.8807; found, 513.8800.

dx.doi.org/10.1021/jm5006435 | J. Med. Chem. 2014, 57, 5792−5799

*3,5-Diiodo-2-methoxy-N-(naphthalen-2-yl)benzamide (**4b**).* Procedure B, 52% yield. ^{1}H NMR (600 MHz, $CDCl_3$) δ 3.95 (s, 3H), 7.42−7.46 (m, 1H), 7.48−7.52 (m, 1H), 7.57 (dd, J = 2.12, 8.75 Hz, 1H), 7.81 (d, J = 8.11 Hz, 1H), 7.83−7.87 (m, 2H), 8.27 (d, J = 2.19 Hz, 1H), 8.38 (d, J = 1.70 Hz, 1H), 8.44 (d, J = 2.19 Hz, 1H), 9.60 (s, 1H). ^{13}C NMR (151 MHz, $CDCl_3$) δ 62.8, 90.1, 93.9, 117.3, 120.0, 125.5, 126.9, 127.8, 127.9, 129.2, 129.4, 131.1, 134.0, 135.2, 141.4, 150.6, 157.2, 161.1. HRMS-ESI (m/z): $[M + H]^+$ calcd for $C_{18}H_{14}I_2NO_2$, 529.9109; found, 529.9114.

*3,5-Diiodo-N-(naphthalen-2-yl)benzamide (**4c**).* Procedure B, 45% yield. ^{1}H NMR (600 MHz, $CDCl_3$) δ 7.44 (ddd, J = 1.09, 6.91, 8.05 Hz, 1H), 7.47−7.51 (m, 1H), 7.57 (dd, J = 2.07, 8.74 Hz, 1H), 7.78−7.86 (m, 3H), 7.89 (s, 1H), 8.17 (d, J = 1.37 Hz, 2H), 8.22 (t, J = 1.46 Hz, 1H), 8.27 (s, 1H). ^{13}C NMR (151 MHz, $CDCl_3$) δ 95.2, 117.6, 120.1, 125.6, 126.9, 127.8, 127.9, 129.2, 131.1, 133.9, 134.8, 135.5, 138.4, 148.4, 162.9. HRMS-ESI (m/z): $[M - H]^-$ calcd for $C_{17}H_{10}I_2NO$, 497.8852; found, 497.8847.

*N-([1,1′-Biphenyl]-4-yl)-2-hydroxy-3,5-diiodobenzamide (**5a**).* Procedure A, 72% yield. ^{1}H NMR (600 MHz, DMSO-d_6) δ 7.36 (t, J = 7.35 Hz, 1H), 7.47 (t, J = 7.72 Hz, 2H), 7.69 (d, J = 7.31 Hz, 2H), 7.72 (d, J = 8.62 Hz, 2H), 7.78 (d, J = 8.64 Hz, 2H), 8.24 (d, J = 1.75 Hz, 1H), 8.43 (d, J = 1.79 Hz, 1H), 10.73 (s, 1H). ^{13}C NMR (151 MHz, DMSO-d_6) δ 81.8, 89.2, 117.5, 122.2, 126.4, 126.9, 127.4, 129.0, 135.9, 136.6, 136.8, 139.5, 149.7, 159.5, 166.9. HRMS-ESI (m/z): $[M + H]^+$ calcd for $C_{19}H_{14}I_2NO_2$, 541.9114; found, 541.9116.

*2-Hydroxy-3,5-diiodo-N-(4′-methyl-[1,1′-biphenyl]-4-yl)-benzamide (**5b**).* Procedure A, 70% yield. ^{1}H NMR (600 MHz, DMSO-d_6) δ 2.34 (s, 3H), 7.27 (d, J = 7.91 Hz, 2H), 7.58 (d, J = 8.03 Hz, 2H), 7.69 (d, J = 8.62 Hz, 2H), 7.76 (d, J = 8.62 Hz, 2H), 8.24 (d, J = 1.65 Hz, 1H), 8.43 (d, J = 1.55 Hz, 1H), 10.70 (s, 1H). ^{13}C NMR (151 MHz, DMSO-d_6) δ 20.7, 81.8, 89.2, 117.5, 122.2, 126.3, 126.6, 129.6, 135.9, 136.5, 136.6, 136.6, 136.6, 149.7, 159.5, 166.8. HRMS-ESI (m/z): $[M + H]^+$ calcd for $C_{20}H_{16}I_2NO_2$, 555.9270; found, 555.9275.

*N-(4′-Chloro-[1,1′-biphenyl]-4-yl)-2-hydroxy-3,5-diiodobenzamide (**5c**).* Procedure A, 68% yield. ^{1}H NMR (600 MHz, DMSO-d_6) δ 7.52 (d, J = 8.46 Hz, 2H), 7.68−7.77 (m, 4H), 7.79 (d, J = 8.61 Hz, 2H), 8.24 (d, J = 1.53 Hz, 1H), 8.42 (d, J = 1.57 Hz, 1H), 10.73 (s, 1H). ^{13}C NMR (151 MHz, DMSO-d_6) δ 81.8, 89.2, 117.5, 122.2, 126.9, 128.2, 128.9, 132.2, 135.2, 135.9, 137.1, 138.3, 149.7, 159.4, 166.9. HRMS-ESI (m/z): $[M + H]^+$ calcd for $C_{19}H_{13}ClI_2NO_2$, 575.8719; found, 575.8735.

*3,5-Diiodo-2-methoxybenzoic Acid (**6b**).* Methyl iodide (0.80 g, 5.6 mmol) was added dropwise to a mixture of 3,5-diiodosalicylic acid (1.0 g, 5.1 mmol) and K_2CO_3 (0.90 g, 6.5 mmol) in acetone (10 mL). After stirring for 3 h at rt, the solvent was removed in vacuo, and the residue was partitioned between H_2O and CH_2Cl_2. The organic layer was separated, and the aqueous phase was extracted with CH_2Cl_2. The organic extracts were concentrated under reduced pressure to give crude methyl 3,5-diiodo-2-methoxybenzoate. The crude product was dissolved in hot methanol (10 mL) to which 1 M KOH (10 mL, 10 mmol) was added. The resulting mixture was heated under reflux for 2 h, diluted with water, and neutralized by addition of 1 M HCl. The product was collected by filtration and recrystallized with ethanol to give **6b** in 61% yield (0.62 g) over two steps. ^{1}H NMR (600 MHz, DMSO-d_6) δ 3.76 (s, 3H), 7.95 (d, J = 2.09 Hz, 1H), 8.30 (d, J = 2.08 Hz, 1H). ^{13}C NMR (151 MHz, DMSO-d_6) δ 61.9, 89.2, 96.6, 128.7, 139.2, 149.2, 158.1, 165.1. HRMS-ESI (m/z): $[M - H]^-$ calcd for $C_8H_5I_2O_3$, 402.8328; found, 402.8325.

*N-Methyl-4-phenoxyaniline (**7**).* Compound **7** was synthesized according to the literature procedure.[34] To a cooled solution of *N*-(4-phenoxyphenyl)acetamide (0.50 g, 2.2 mmol) in anhydrous THF (5 mL) was added NaH (97 mg, 2.4 mmol, 60% dispersion in mineral oil). After stirring for 5 min, MeI (0.20 mL, 3.2 mmol) was added dropwise, and the resulting mixture was stirred for 1 h at rt and then partitioned between H_2O and CH_2Cl_2. The organic phase was separated and the aqueous layer was extracted with CH_2Cl_2. Concentration of the combined organic extracts in vacuo gave the crude *N*-methyl-*N*-(4-phenoxyphenyl)acetamide, which was used in the next step without further purification. Concentrated HCl (0.5 mL) was added to a stirred solution of crude *N*-methyl-*N*-(4-phenoxyphenyl)acetamide in ethylene glycol (3 mL). The mixture was heated under reflux overnight, diluted with H_2O, and extracted with EtOAc. The organic layers were combined, dried over anhydrous Na_2SO_4, and concentrated under reduced pressure. Purification of the crude product by silica chromatography gave compound **7** in 56% yield (0.25 g) over two steps. ^{1}H NMR (600 MHz, $CDCl_3$) δ 2.85 (s, 3H), 6.61−6.65 (m, 2H), 6.94−6.98 (m, 4H), 7.03 (t, J = 7.35 Hz, 1H), 7.30 (t, J = 7.96 Hz, 2H). ^{13}C NMR (151 MHz, $CDCl_3$) δ 31.4, 113.5, 117.1, 121.4, 122.0, 129.6, 146.1, 147.6, 159.3. HRMS-ESI (m/z): $[M + H]^+$ calcd for $C_{13}H_{14}NO$, 200.1075; found, 200.1069.

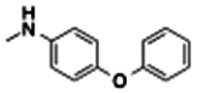

7

*N-(2-(1H-Indol-3-yl)ethyl)-2-hydroxy-3,5-diiodobenzamide (**8**).* Procedure A, 65% yield. ^{1}H NMR (500 MHz, DMSO-d_6) δ 2.97 (t, J = 7.45 Hz, 2H), 3.57 (q, J = 7.04 Hz, 2H), 6.94−7.02 (m, 1H), 7.03−7.11 (m, 1H), 7.18 (d, J = 2.21 Hz, 1H), 7.34 (d, J = 8.09 Hz, 1H), 7.55 (d, J = 7.86 Hz, 1H), 8.14−8.23 (m, 2H), 9.28 (t, J = 5.43 Hz, 1H), 10.84 (s, 1H). ^{13}C NMR (151 MHz, DMSO-d_6) δ 24.6, 40.3, 81.4, 88.8, 111.4, 111.5, 116.3, 118.2, 118.3, 121.0, 122.8, 127.1, 135.2, 136.2, 149.3, 159.9, 168.0. HRMS-ESI (m/z): $[M + H]^+$ calcd for $C_{17}H_{14}I_2N_2O_2$, 532.9218; found, 532.9208.

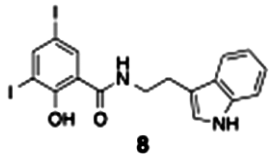

8

Chitinase Inhibition. Chitinase activity assay was performed as previously described.[12]

Mitochondrial-Uncoupling Assays. Adherent human epithelial kidney cells [HEK 293T/17] (ATCC CRL-11268) were trypsinized and resuspended in 10% FBS in DMEM at a density of 1−2 × 10^6 cells/mL. Cells were incubated with DMSO (blank control) or 50 μM compound for 30 min at 37 °C. Tetramethylrhodamine ethyl ester perchlorate (TMRE, ∼450 nM final concentration) was added, followed by incubation in the dark for 30 min at 37 °C. Cells were washed twice with 0.2% BSA in PBS, centrifuged, and resuspended in 0.2% BSA in PBS. For the microplate assay, fluorescence signals were measured using a SpectraMaxM2e microplate reader (Molecular Devices, Sunnyvale, CA) (λ_{ex} = 549 nm, λ_{em} = 575 nm). For flow cytometry, 1−2 × 10^6 cells per sample were collected using DIVA 6.0 software on an LSRII flow cytometer (BD Biosciences, San Jose, CA). FACS data was further analyzed using FlowJo software (Tree Star, Inc., Ashland, OR).

***C. elegans* Culture.** *C. elegans* growth and maintenance were performed using standard protocols.[35]

Bioaccumulation in *C. elegans*. The procedure for the small molecule accumulation assay was adapted from Burns et al.[21] Briefly, synchronized worms were grown to late-stage L4 worms at 25 °C on *Escherichia coli* OP50 for 40 h. Worms were harvested, washed three times with water, and resuspended in M9 buffer to a final concentration of ∼5−10 worms/μL. To 200 μL of the worm suspension was added 2 μL of 1 mM compound in DMSO (equivalent to ∼2 nmol/mg worm). After incubation for 6 h (or 12 h) at rt, the worms were washed with 500 μL of 0.1% SDS, followed by three 500 μL washes with water. After washing, the worms were flash frozen in liquid nitrogen, lyophilized, weighed, and stored at −80 °C until analyses.

Sample Analysis. Worms were homogenized for 5 min in a 100-volume equivalent of cold methanol/acetonitrile mixture (1:1) containing 500 nM internal standard **8**, using a bullet blender (Next Advance, Inc., Averill Park, NY). After centrifugation for 10 min at 4 °C, the supernatants were collected and analyzed by reversed-phase

dx.doi.org/10.1021/jm5006435 | *J. Med. Chem.* 2014, 57, 5792−5799

LC with MS detection (mass filter at m/z = 589.846−589.856 for **3h**, m/z = 605.878−605.888 for **3i**, m/z = 623.807−623.817 for **3m**, m/z = 513.875−513.885 for **4a**, and m/z = 529.906−529.916 for **4b**). Standard calibration curves were prepared by fortification of blank worms with compounds **3h**, **3i**, **3m**, **4a**, and **4b** at concentrations up to 2 nmol/mg worm. The concentrations in worms were quantified using peak area ratios relative to the internal standard and linear regression parameters were calculated from the calibration curve standards prepared in blank worms.

Liquid Chromatography and Mass Spectrometry. The LC system consisted of Agilent 1200 LC (Agilent Technologies, Santa Clara, CA) equipped with an autosampler and a column heater. Mass spectrometric experiments were performed with Agilent TOF 6210 and monitored with Mass Hunter qualitative analysis software, version B.03.01 (Agilent Technologies, Santa Clara, CA). Mass spectrometry acquisition was performed using electrospray ionization with the following parameters: capillary voltage = 3.5 kV, nebulizer pressure = 20 psig, drying gas flow = 7 L/min, and gas temperature = 350 °C. Samples were analyzed on a Poroshell 120 EC-C8 column (2.7 μm, 2.1 mm i.d. 100 mm, Agilent, USA). The mobile phase consisted of elution at 0.20 mL/min starting with an 8 min linear gradient from 70% A/30% B to 100% B and then 100% B for 12 min (positive-ESI, A = 0.1% formic acid in water, B = 0.1% formic acid in acetonitrile; negative-ESI, A = water, B = acetonitrile).

***O. volvulus* L3 Molting Inhibition.** Experiments using *O. volvulus* L3 larvae in molting assay were the same as described previously[12] except that the larvae were incubated with the compounds for 24 h prior to addition of the complete medium (containing 20% heat inactivated FCS) and normal PBMCs.

Cell Viability Assay. HEK 293T/17 cells (2×10^4 cells) were plated in 96-well plates and incubated at 37 °C for 24 h. Cells were then treated with compounds **3h**, **3m**, and **4a** (at a final concentration of 1 and 10 μM), and an MTS assay was performed at 0.5 and 24 h postincubation using the CellTiter 96 aqueous non-radioactive cell proliferation assay (Promega, Madison, WI) per manufacturer's instructions.

■ ASSOCIATED CONTENT

Ⓢ Supporting Information

Activity of chitinases from different species, evaluation of mitochondrial-uncoupling by fluorescence spectrometry and flow cytometry, metabolism of closantel in *C. elegans*, and cell viability after treatment with compounds **3h**, **3m**, and **4a**. This material is available free of charge via the Internet at http://pubs.acs.org.

■ AUTHOR INFORMATION

Corresponding Author

*Phone: (858) 785-2515. Fax: (858) 784-2595. E-mail: kdjanda@scripps.edu.

Notes

The authors declare no competing financial interest.

■ ACKNOWLEDGMENTS

This work was supported by NIH grant AI092076. We thank Greg McElhaney for preparation of compounds **5a**−**c**.

■ ABBREVIATIONS USED

O. volvulus, *Onchocherca volvulus*; OvCHT1, *Onchocherca volvulus* chitinase; L3, third larval stage; L4, fourth larval stage; CCCP, *C. elegans*, *Caenorhabditis elegans*; LC, liquid chromatography; MS, mass spectrometry

■ REFERENCES

(1) Allen, J. E.; Adjei, O.; Bain, O.; Hoerauf, A.; Hoffmann, W. H.; Makepeace, B. L.; Schulz-Key, H.; Tanya, V. N.; Trees, A. J.; Wanji, S.; Taylor, D. W. Of mice, cattle, and humans: the immunology and treatment of river blindness. *PLoS Negl. Trop. Dis.* **2008**, *2*, e217.

(2) Omura, S.; Crump, A. The life and times of ivermectin—a success story. *Nature Rev. Microbiol.* **2004**, *2*, 984−989.

(3) Awadzi, K.; Attah, S. K.; Addy, E. T.; Opoku, N. O.; Quartey, B. T.; Lazdins-Helds, J. K.; Ahmed, K.; Boatin, B. A.; Boakye, D. A.; Edwards, G. Thirty-month follow-up of sub-optimal responders to multiple treatments with ivermectin, in two onchocerciasis-endemic foci in Ghana. *Ann. Trop. Med. Parasitol.* **2004**, *98*, 359−370.

(4) Basanez, M. G.; Pion, S. D.; Boakes, E.; Filipe, J. A.; Churcher, T. S.; Boussinesq, M. Effect of single-dose ivermectin on *Onchocerca volvulus*: a systematic review and meta-analysis. *Lancet Infect. Dis.* **2008**, *8*, 310−322.

(5) Lustigman, S.; McCarter, J. P. Ivermectin resistance in *Onchocerca volvulus*: toward a genetic basis. *PLoS Negl. Trop. Dis.* **2007**, *1*, e76.

(6) Osei-Atweneboana, M. Y.; Eng, J. K.; Boakye, D. A.; Gyapong, J. O.; Prichard, R. K. Prevalence and intensity of *Onchocerca volvulus* infection and efficacy of ivermectin in endemic communities in Ghana: a two-phase epidemiological study. *Lancet* **2007**, *369*, 2021−2029.

(7) Spindler, K. D.; Spindler-Barth, M.; Londershausen, M. Chitin metabolism: a target for drugs against parasites. *Parasitol. Res.* **1990**, *76*, 283−288.

(8) Adam, R.; Kaltmann, B.; Rudin, W.; Friedrich, T.; Marti, T.; Lucius, R. Identification of chitinase as the immunodominant filarial antigen recognized by sera of vaccinated rodents. *J. Biol. Chem.* **1996**, *271*, 1441−1447.

(9) Arnold, K.; Brydon, L. J.; Chappell, L. H.; Gooday, G. W. Chitinolytic activities in *Heligmosomoides polygyrus* and their role in egg hatching. *Mol. Biochem. Parasitol.* **1993**, *58*, 317−323.

(10) Tachu, B.; Pillai, S.; Lucius, R.; Pogonka, T. Essential role of chitinase in the development of the filarial nematode *Acanthocheilonema viteae*. *Infect. Immun.* **2008**, *76*, 221−228.

(11) Wu, Y.; Egerton, G.; Underwood, A. P.; Sakuda, S.; Bianco, A. E. Expression and secretion of a larval-specific chitinase (family 18 glycosyl hydrolase) by the infective stages of the parasitic nematode *Onchocerca volvulus*. *J. Biol. Chem.* **2001**, *276*, 42557−42564.

(12) Gloeckner, C.; Garner, A. L.; Mersha, F.; Oksov, Y.; Tricoche, N.; Eubanks, L. M.; Lustigman, S.; Kaufmann, G. F.; Janda, K. D. Repositioning of an existing drug for the neglected tropical disease Onchocerciasis. *Proc. Natl. Acad. Sci. U. S. A.* **2010**, *107*, 3424−3429.

(13) Van Den Bossche, H.; Verhoeven, H.; Vanparijs, O.; Lauwers, H.; Thienpont, D. Closantel, a new antiparasitic hydrogen ionophore [proceedings]. *Arch. Int. Physiol. Biochim.* **1979**, *87*, 851−853.

(14) Segura-Cabrera, A.; Bocanegra-Garcia, V.; Lizarazo-Ortega, C.; Guo, X.; Correa-Basurto, J.; Rodriguez-Perez, M. A. A computational analysis of the binding mode of closantel as inhibitor of the *Onchocerca volvulus* chitinase: insights on macrofilaricidal drug design. *J. Comput.-Aided Mol. Des.* **2011**, *25*, 1107−1119.

(15) van Aalten, D. M.; Komander, D.; Synstad, B.; Gaseidnes, S.; Peter, M. G.; Eijsink, V. G. Structural insights into the catalytic mechanism of a family 18 exo-Chitinase. *Proc. Natl. Acad. Sci. U. S. A.* **2001**, *98*, 8979−8984.

(16) Armour, J.; Corba, J. The anthelmintic activity of rafoxanide against immature *Fasciola hepatica* in sheep. *Vet. Rec.* **1970**, *87*, 213−214.

(17) Horton, D. A.; Bourne, G. T.; Smythe, M. L. The combinatorial synthesis of bicyclic privileged structures or privileged substructures. *Chem. Rev.* **2003**, *103*, 893−930.

(18) Cox, G. N.; Kusch, M.; Edgar, R. S. Cuticle of *Caenorhabditis elegans*: its isolation and partial characterization. *J. Cell Biol.* **1981**, *90*, 7−17.

(19) Selkirk, M. E.; Nielsen, L.; Kelly, C.; Partono, F.; Sayers, G.; Maizels, R. M. Identification, synthesis and immunogenicity of cuticular collagens from the filarial nematodes *Brugia malayi* and *Brugia pahangi*. *Mol. Biochem. Parasitol.* **1989**, *32*, 229−246.

(20) Lustigman, S.; Huima, T.; Brotman, B.; Miller, K.; Prince, A. M. *Onchocerca volvulus*: biochemical and morphological characteristics of the surface of third- and fourth-stage larvae. *Exp. Parasitol.* **1990**, *71*, 489−495.

(21) Burns, A. R.; Wallace, I. M.; Wildenhain, J.; Tyers, M.; Giaever, G.; Bader, G. D.; Nislow, C.; Cutler, S. R.; Roy, P. J. A predictive model for drug bioaccumulation and bioactivity in *Caenorhabditis elegans*. *Nature Chem. Biol.* **2010**, *6*, 549−557.
(22) Lindblom, T. H.; Dodd, A. K. Xenobiotic detoxification in the nematode *Caenorhabditis elegans*. *J. Exp. Zool., Part A* **2006**, *305*, 720−730.
(23) Michiels, M.; Meuldermans, W.; Heykants, J. The metabolism and fate of closantel (Flukiver) in sheep and cattle. *Drug Metab. Rev.* **1987**, *18*, 235−251.
(24) Strote, G.; Bonow, I. Morphological demonstration of essential functional changes after in vitro and in vivo transition of infective *Onchocerca volvulus* to the post-infective stage. *Parasitol. Res.* **1991**, *77*, 526−535.
(25) Marchand, C. The elvitegravir Quad pill: the first once-daily dual target anti-HIV tablet. *Expert Opin. Invest. Drugs* **2012**, *12*, 901−904.
(26) Flaherty, K. T.; Infante, J. R.; Daud, A.; Gonzalez, R.; Kefford, R. F.; Sosman, J.; Hamid, O.; Schuchter, L.; Cebon, J.; Ibrahim, N.; Kudchadkar, R.; Burris, H. A., III; Falchook, G.; Algazi, A.; Lewis, K.; Long, G. V.; Puzanov, I.; Lebowitz, P.; Singh, A.; Little, S.; Sun, P.; Allred, A.; Ouellet, D.; Kim, K. B.; Patel, K.; Weber, J. Combined BRAF and MEK inhibition in melanoma with BRAF V600 mutations. *N. Engl. J. Med.* **2012**, *367*, 1694−1703.
(27) Priotto, G.; Kasparian, S.; Mutombo, W.; Ngouama, D.; Ghorashian, S.; Arnold, U.; Ghabri, S.; Baudin, E.; Buard, V.; Kazadi-Kyanza, S.; Ilunga, M.; Mutangala, W.; Pohlig, G.; Schmid, C.; Karunakara, U.; Torreele, E.; Kande, V. Nifurtimox−eflornithine combination therapy for second-stage African *Trypanosoma brucei gambiense* trypanosomiasis: a multicentre, randomised, phase III, non-inferiority trial. *Lancet* **2009**, *374*, 56−64.
(28) Sinclair, D.; Zani, B.; Donegan, S.; Olliaro, P.; Garner, P. Artemisinin-based combination therapy for treating uncomplicated malaria. *Cochrane Database Syst. Rev.* **2009**, 3, CD007483.
(29) Ciceri, P.; Muller, S.; O'Mahony, A.; Fedorov, O.; Filippakopoulos, P.; Hunt, J. P.; Lasater, E. A.; Pallares, G.; Picaud, S.; Wells, C.; Martin, S.; Wodicka, L. M.; Shah, N. P.; Treiber, D. K.; Knapp, S. Dual kinase−bromodomain inhibitors for rationally designed polypharmacology. *Nature Chem. Biol.* **2014**, *10*, 305−312.
(30) Katsoulas, A.; Rachid, Z.; McNamee, J. P.; Williams, C.; Jean-Claude, B. J. Combi-targeting concept: an optimized single-molecule dual-targeting model for the treatment of chronic myelogenous leukemia. *Mol. Cancer Ther.* **2008**, *7*, 1033−1043.
(31) Tari, L. W.; Li, X.; Trzoss, M.; Bensen, D. C.; Chen, Z.; Lam, T.; Zhang, J.; Lee, S. J.; Hough, G.; Phillipson, D.; Akers-Rodriguez, S.; Cunningham, M. L.; Kwan, B. P.; Nelson, K. J.; Castellano, A.; Locke, J. B.; Brown-Driver, V.; Murphy, T. M.; Ong, V. S.; Pillar, C. M.; Shinabarger, D. L.; Nix, J.; Lightstone, F. C.; Wong, S. E.; Nguyen, T. B.; Shaw, K. J.; Finn, J. Tricyclic GyrB/ParE (TriBE) inhibitors: a new class of broad-spectrum dual-targeting antibacterial agents. *PloS One* **2013**, *8*, e84409.
(32) Harrison, R. A.; Wu, Y.; Egerton, G.; Bianco, A. E. DNA immunisation with *Onchocerca volvulus* chitinase induces partial protection against challenge infection with L3 larvae in mice. *Vaccine* **1999**, *18*, 647−655.
(33) Endres, A.; Maas, G. Dirhodium (II) tetrakis-(perfluoroalkylbenzoates) as partially recyclable catalysts for carbene transfer reactions with diazoacetates. *Tetrahedron* **2002**, *58*, 3999−4005.
(34) Peng, Y.; Liu, H.; Tang, M.; Cai, L.; Pike, V. Highly efficient *N*-monomethylation of primary aryl amines. *Chin. J. Chem.* **2009**, *27*, 1339−1344.
(35) Lewis, J. A.; Fleming, J. T. Basic Culture Methods. In *Caenorhabditis Elegans: Modern Biological Analysis of an Organism*; Epstein, H. F., Shakes, D. C., Eds.; Academic Press: San Diego, CA, 1995; pp 4−27.